LOW-SPEED PERMANENT-MAGNET SYNCHRONOUS GENERATOR FOR SMALL-SCALE WIND POWER APPLICATIONS

A. KILK[*]

Department of Fundamentals of Electrical Engineering and Electrical Machines
Tallinn University of Technology
5 Ehitajate Rd., 19086 Tallinn, Estonia

Tendencies in development of wind power industry including direct-drive small-scale wind power plants and generators have been analyzed. Synchronous generators with permanent magnet excitation for direct-drive wind power turbines are described. Primary magnetic field distribution and effect of armature reaction have been studied for design of a low-speed multipole permanent-magnet synchronous generator with radial magnetic flux. The test results of a prototype permanent-magnet generator are analyzed and compared with the calculated data and characteristics.

Introduction

Wind power is an energy source whose industrial application in the world has grown at the fastest rate in the last 10–15 years. Installed capacity of wind power plants is continuously growing at a level of annual rate exceeding 30%. The European power market has been the main driving force in development of wind power industry for many years. In EU countries, a record installation of more than 6 180 MW new wind power generators was achieved in 2005. By the end of 2005, the capacity of wind energy generation reached a level of more than 40 500 MW in Europe and more than 59 300 MW worldwide [1]. In Europe, the current targets of using wind capacity are 75 000 MW by 2010, 180 000 MW by 2020, and 300 000 MW by 2030.

Powerful grid-connected megawatt-scale wind generators 0.5–5.0 MW per unit are mostly manufactured and installed as pollution-free sources of renewable energy in the world in last years. At the same time many smaller wind turbines are required for certain installations and local consumption as maintenance-free independent power suppliers. A small-scale wind power

---

[*] Corresponding author: e-mail address *kilk@cc.ttu.ee*

turbine of the capacity 0.2–30 kW, with rotor diameters from 1 m up to 15 m may be used as a flexible and vital alternative for local power demand in isolated regions or locations [2–4].

Permanent-magnet (PM) synchronous generators are one of the best solutions for small-scale wind power plants. Low-speed multipole PM generators are maintenance-free and may be used in different climate conditions. It is possible to combine PM wind generators for hybride technologies such as wind-diesel, wind-photovoltaic etc.

A conventional megawatt-scale wind power plant consists of a low-speed wind turbine rotor, gearbox and high-speed (1000–1500 rpm) electric generator (Fig. 1*a*). The rotor of a typical wind turbine rotates at the speed of 15–100 rpm (150–500 rpm for small-scale wind turbines) [4].
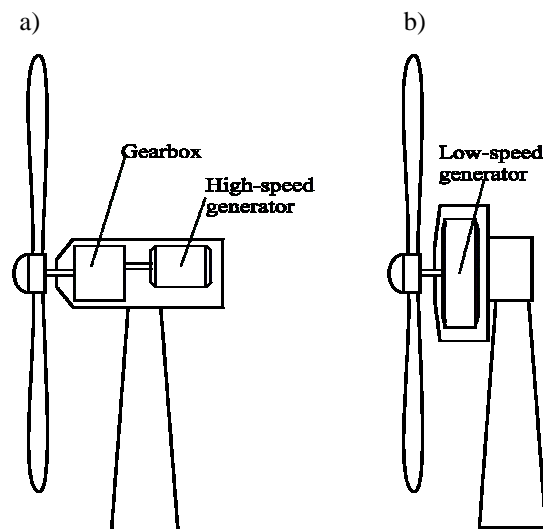

Fig. 1. Typical structures of gearbox-generator (*a*) and direct-drive generator (*b*) of a wind power plant.

The use of a gearbox causes many technological problems in a wind power plant, as it demands regular maintenance, increases the weight of the wind plant, generates noise and increases power losses. These problems may be avoided using an alternative – a direct-drive low-speed PM synchronous generator (Fig. 1*b*) [4, 5].

This paper studies small-scale synchronous generators with permanent magnet excitation for direct-drive wind-power turbines and presents the analysis of magnetic field distribution in air gap and in magnetic circuit of the generator with radial magnetic flux and permanent magnet excitation. The results of analytical as well as experimental study of low-speed direct-

drive permanent magnet-excited synchronous generators for small-scale wind power applications have been presented.

Low-speed direct-drive permanent magnet synchronous generators

In small-scale wind power plants very often low-speed direct-drive synchronous generators are used. Due to low rotational speed of the synchronous generator directly connected to the mechanical shaft of the wind rotor, the generator has a multipole construction [3, 5]. In this paper an electromagnetic analysis of a low-speed direct-drive multipole synchronous generator for wind power applications of 5–10 kW power level is presented.

A synchronous generator may be excited by traditional current-carrying field winding or by permanent magnet system of high energy. Synchronous generators with permanent magnet excitation for small-scale wind power units are more maintenance-free and reliable in long-term exploitation [2–4]. Due to high number of pole pairs, the PM construction enables a mass reduction in the stator yoke and rotor back-iron. As a result, the development of those innovative low-speed synchronous generators with PM excitation has been received high attention in the world for the last decade.

A series of low-speed direct-drive synchronous generators of the rated power of 5–10 kW with PM excitation was used in the frames of the present study. The generators were of a conventional construction of a typical synchronous generator with radial magnetic flux in the air gap between the inner rotor and the outer stator. The radial-flux PM generators may be divided into two main groups: with surface-magnet or buried-magnet systems [2, 4], respectively. In this study PM generators with the surface-magnet system have been studied and analyzed.

Analysis of primary magnetic field in PM synchronous generators

The primary magnetic field caused by PM poles of a synchronous generator have been modelled as well as analyzed by the method of conformal mapping. The construction of PM poles may be designed with or without ferromagnetic pole shoes. In this paper distribution of the magnetic field caused by PM poles both with and without ferromagnetic shoes has been studied.

A linear model of the PM synchronous generator for analysis of magnetic flux distribution in the non-magnetic gap between ferromagnetic cores of the armature and inductor has been created for this study (Fig. 2). This model was used to describe the distribution of magnetic flux caused by permanent magnets to main flux Φ_{01} and leakage flux Φ_s.
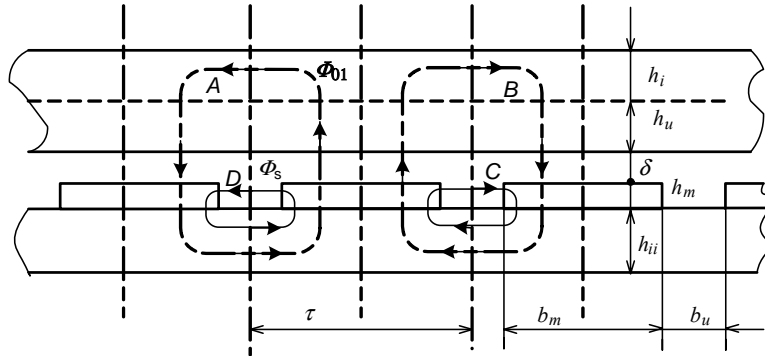
Fig. 2. A linear model of the air-gap zone for a PM synchronous generator.

Magnetic field in the air gap of the PM synchronous generator with ferromagnetic pole shoes

Distribution of the primary magnetic field in the air gap of the radial-flux PM synchronous generator has been analyzed by means of an analytical model created for the PM machine topology, in which the following assumptions are used:

1) Stator surface is toothless and smooth (salience of the stator surface is neglected), the influence of slots will be considered by Carter factor.
2) Magnetic scalar potential U_m of the ferromagnetic pole shoes on the N-pole magnet surface $U_{m1} = +F_m$, that on the S-pole magnet surface $U_{m2} = -F_m$, and on the stator surface $U_{m3} = 0$ (Fig. 3).

To determine the distribution of magnetic field in the air gap, the method of conformal mapping has been used [5, 6]. The linear model of the air gap between the surfaces of a pair of N–S magnets covered by ferromagnetic shoes and stator's ferromagnetic core of a PM generator (Fig. 4a) is presented in complex coordinates $z = x + jy$ as the zone $z_1 - z_2 - z_3 - z_4 - z_5$. The depth of the gap between PM poles is indefinite.

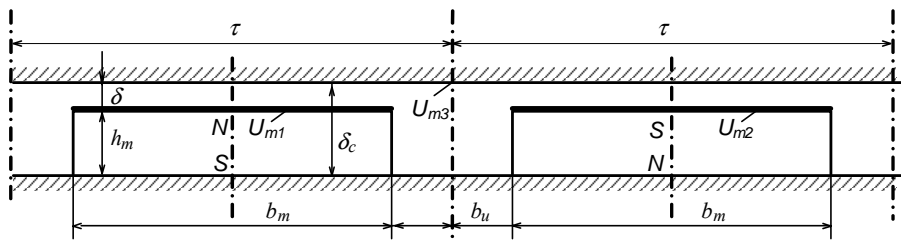The zone of respective conformal complex coordinates $w = u + jv$ is presented in Fig. 4b.

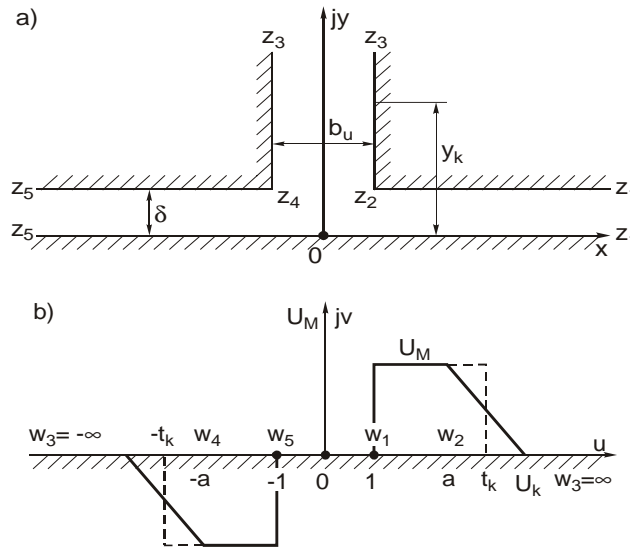*Fig. 3*. A linear model of the air gap zone for PM poles with ferromagnetic shoes.

Fig. 4. Air gap model of the PM generator (*a*),
and the conformal map of the model (*b*).

Using the conformal mapping method and considering the boundary conditions of magnetic scalar potential U_m for the magnet-pole and stator surfaces in *z*-coordinates, at first the magnetic complex potential $W(w)$ for the conformal complex *w*-coordinates may be determined by Schwarz' integral [5, 6]. As a result of integrating, the equation for the conformal function of the magnetic complex potential $W(w)$ in the zone of air gap in *w*-coordinates will be obtained.

Magnetic flux density in *w*-coordinates will be evaluated as a derivative of the magnetic vector potential $W(w)$

$$\overline{B}_w = -j\mu_0 \frac{d\overline{W}(w)}{dw}. \tag{1}$$

On the basis of magnetic flux density in *w*-coordinates, the distribution of magnetic flux density in *z*-coordinates (in the air gap) will be obtained:

$$\overline{B}_z = \overline{B}_w \left(\overline{\frac{dw}{dz}} \right). \tag{2}$$

Magnetic flux density in the air gap for the stator's core surface can be expressed as

$$\overline{B}_z^{''} = -jB_a \frac{2\delta}{b_u} \frac{\overline{w}}{\sqrt{a^2 - \overline{w}^2}}. \tag{3}$$

Distribution of magnetic flux density in the air gap on the surface of the stator core without slots for one pole pitch calculated by Eq. (3) is presented in Fig 5.
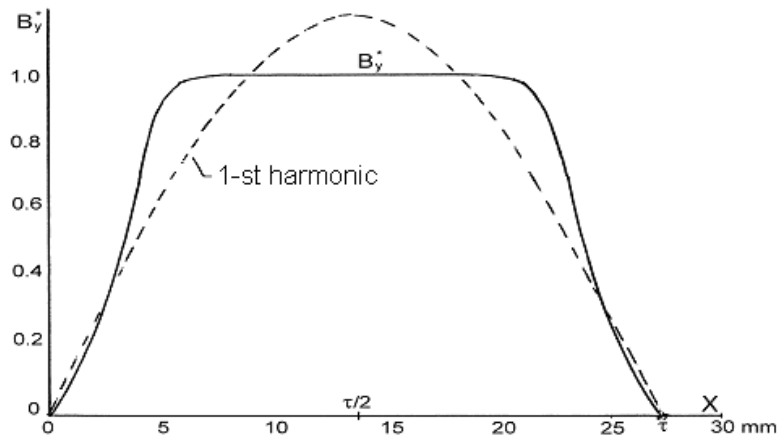

Fig. 5. Distribution of magnetic flux density in the air gap of the PM generator on the surface of stator core without slots for pole pitch at constant length of the air gap.

As a result of Fourier' analysis of the computed distribution of magnetic flux density using Eq. (3), the curve of the 1st harmonic of magnetic flux density has been calculated and shown in Fig. 3. As can be noticed by comparison of the curves of total and the 1st harmonic of flux density in Fig. 5, the curve of total magnetic flux density $B_y^*(x)$ is considerably influenced by the 3rd harmonic.

Integration of magnetic flux density B_y^* per one pole pitch will give the value of total magnetic flux in the air gap per one pole as

$$\phi_\delta = \mu_0 \frac{F_m}{\delta} \tau \, l_m k_\phi \,, \tag{4}$$

where l_m – length of stator's magnetic core; k_ϕ – coefficient of magnetic flux reduction obtained by conformal mapping (for the curve of magnetic flux density in Fig. 5 the coefficient k_ϕ will be $k_\phi = 0.756$).

Magnetic field in the air gap of the PM synchronous generator without ferromagnetic pole shoes

For analytical analysis of distribution of the primary magnetic field in the air gap, a model for a non-magnetic gap including the zones of both air gap and permanent magnets between the armature and ferromagnetic surfaces of the inductor was created. Instead of permanent magnets, a system of linear-surface current densities $\pm\sigma_s$ has been included in the model (Fig. 6).
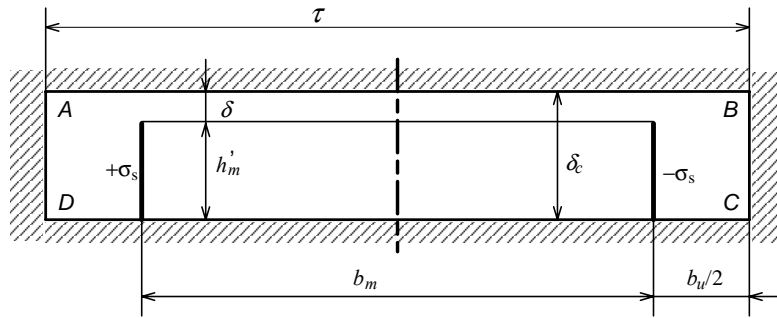
Fig. 6. A model of an equivalent non-magnetic gap of the PM generator.

For the zone A-B-C-D of the model, distribution of magnetic field caused by surface current densities $\pm\sigma_s$ may be determined by solving Maxwell equations. However, it will be complicated to use this solution for practical calculations in the cases of different constructions of PM synchronous generators.

In the present study the method of conformal mapping has been used for analysis of the magnetic field distribution. A model for one half of a PM pole zone for the plane $z = x + jy$ has been created (Fig. 7*a*). As the result of conformal mapping, this model will be transformed into a new model for the plane $w = u + jv$ (Fig. 7*b*).
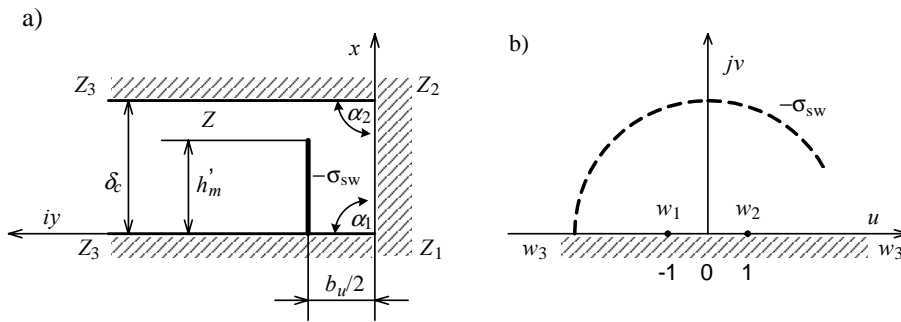

Fig. 7. Conformal mapping of the model for the air gap of the PM generator.

By means of conformal mapping method distribution of primary magnetic flux density in the air gap was determined at first for the w-plane B_w, and thereafter transformed to the real z-plane B_z:

$$B_z = B_a \sqrt{|u^2 - 1|} \frac{1}{n} \sum_{i=1}^{n} \frac{(u - u_{si})}{(u - u_{si})^2 + v_{si}^2} , \qquad (5)$$

where the calculated value of magnetic flux density in the air gap on the axis of permanent magnets

$$B_a = \mu_0 \frac{I}{\delta_c} = \mu_0 \frac{F_c}{\delta_c}, \qquad (6)$$

and the calculated magnetomotive force of permanent magnets by rated temperature

$$F_c = H_c \cdot h_m. \qquad (7)$$

Distribution of relative magnetic flux density in the air gap on the level of the stator's core surface calculated by these equations was compared by experimental data (Fig. 8). There was a good correlation between calculated and experimental data.

As a result of this analysis, the distribution of main magnetic flux in the air gap and magnetic cores of both armature and inductor will be calculated. At the same time the distribution of leakage flux will be taken into consideration.
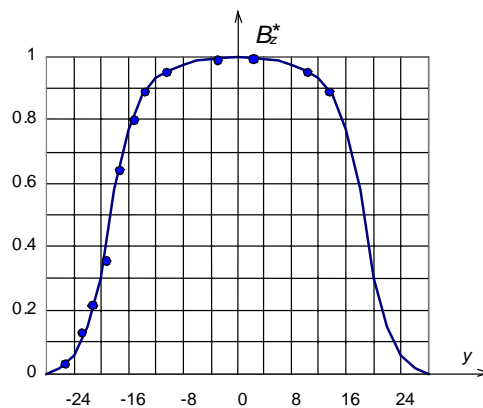

Fig. 8. Calculated and experimental distribution of relative magnetic flux density in the air gap on the surface of the armature core.

Analysis of magnetic flux distribution by the method of equivalent magnetic circuits

For simplified analysis of both main and leakage fluxes, the method of equivalent lumped-parameter magnet circuit in accordance with the topology of the PM generator may be used (Fig. 9).

To calculate a more exact distribution of magnetic fluxes from the permanent magnet into the air gap of the machine, the surface of the magnet has been divided into two parts causing two different paths of leakage fluxes
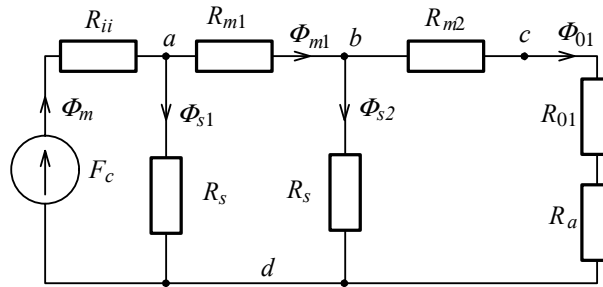
Fig. 9. A lumped-parameter magnetic circuit for the PM synchronous generator.

Φ_{s1} and Φ_{s2} respectively. Using this method, the main magnetic flux Φ_{01} as well as the distribution of the primary magnetic field was calculated for comparison.

For design of a PM generator, the influence of the air gap of varying thickness between PM poles and stator core surfaces has been analyzed to determine the way how to transform it to an equivalent air gap of constant thickness. As a result, some corrections have been developed for design calculations of PM synchronous generators.

Armature reaction in PM generators

Under load conditions the currents in the armature winding of the PM generator will create the secondary magnetic field, which will cause the armature to react affecting the resulting magnetic field. Armature reaction will cause a distortion of the distribution of the magnetic field in the air gap of the PM generator. The *d*- and *q*-axis components of armature reaction have been studied.

The *d*-axis component of armature reaction by the direction of permanent magnet axis will affect the strength of the primary magnetic field in the air gap (Fig. 10*a*). The *q*-axis component of armature reaction by the direction of the axis between permanent magnets will, first of all, cause a distortion of the primary magnetic field in the air gap (Fig. 11*a*).

The level of permeability μ_s of permanent magnet materials is very low. As a result, the equivalent thickness of the air gap δ_{eqv} (different for *d*- and *q*-axis) will be much larger than δ_0. It will reduce relatively the effect of armature reaction on the magnetic field in the air gap compared to conventional synchronous machines of traditional construction.

The magnets are placed and fixed in nests on the rotor surface. The distribution of both *d*- and *q*-axis magnetic flux components of radial-flux PM synchronous generator and equivalent magnetic circuit diagrams for calculation of magnetic fluxes are shown in Fig. 6 and Fig. 7, respectively.
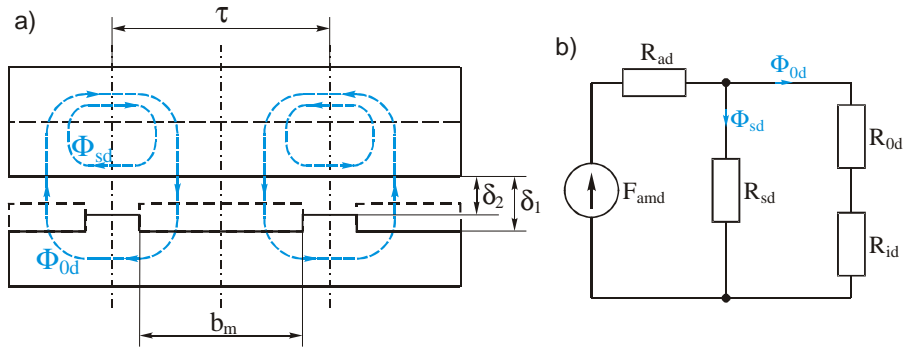
Fig. 10. Distribution of d-axis magnetic fluxes of armature reaction (*a*) and equivalent magnetic circuit diagram (*b*) for calculation of d-axis magnetic fluxes.
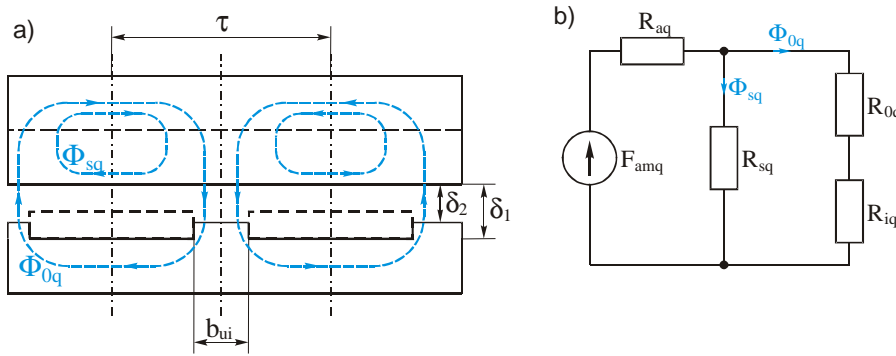

Fig. 11. Distribution of q-axis magnetic fluxes of armature reaction (*a*) and equivalent magnetic circuit diagram (*b*) for calculation of q-axis magnetic fluxes.

At analysing magnetic flux distribution of armature reaction for *d*-axis, the expression for resulting magnetic flux per one pole pitch τ in *d*-axis was obtained as follows:

$$\phi_d = \mu_0 \frac{2}{\pi} \frac{F_{amd}}{k_{ci} \cdot k_{\mu d} \delta_1} l_m \tau \cdot k_{\phi d}, \tag{13}$$

where $k_{\phi d}$ is the magnetic flux coefficient of armature reaction for *d*-axis

$$k_{\phi d} = \left(1 - \frac{k_{c1} \cdot \delta_1}{k_{c2} \cdot \delta_2}\right) \sin\left(\frac{b_m}{\tau} \frac{\pi}{2}\right) + \frac{k_{c1} \delta_1}{k_{c2} \delta_2}. \tag{14}$$

The formulae for calculation of magnetic flux of armature reaction for *q*-axis can be expressed as

$$\phi_{aq} = \mu_0 \frac{2}{\pi} \frac{F_{amq}}{k_{c2} k_{\mu q} \delta_2} \tau l_m k_{\phi q} , \tag{15}$$

where $k_{\Phi q}$ is the magnetic flux coefficient of armature reaction for q-axis:

$$k_{\phi q} = \left(1 - \frac{k_{c2} \delta_2}{k_{c1} \delta_1} \right) \cos \left(\frac{b_m}{\tau} \frac{\pi}{2} \right) + \frac{k_{c2} \delta_2}{k_{ci} \delta_1} . \tag{16}$$

Because of the *q*-axis component of armature reaction, first of all, distortion of the magnetic field in the teeth and yoke zone of the armature will be caused. The *q*-axis component of magnetic flux related to the inductor and permanent magnets is relatively small. The *d*-axis component of armature reaction will cause reduction of magnetic flux density by about 12–15% in the teeth zone of the armature core at rated load currents. As the result, both *q*- and *d*-axis components of armature reaction cause a 17-% reduction of magnetic flux in the teeth zone. In this reduction, the influence of slot leakage flux has been taken into account.

Due to very low permeability μ_s for permanent magnet material, the equivalent thickness of a non-magnetic gap between the armature and magnetic cores of the inductor is relatively large. The influence of a large non-magnetic gap will reduce the effect of armature reaction in PM generators compared to conventional synchronous machines [5].

Design and experimental study of the PM generator

A prototype of the 10-kW PM synchronous generator with fractional two-layer armature winding was designed using analytical methods and results of conformal mapping studies. For comparison the distribution of magnetic fields was analyzed by the finite element method using the program Maxwell.

For the prototype PM machine, the number of armature slots 60 and the number of pole pairs 14 were chosen. Rectangular NdFeB magnets were fixed in the nests on the radial surface of the inductor's magnetic core. The length and outer diameter of the air gap were 240 mm and 242 mm, respectively. The line voltage in open-circuit conditions 488 V, nominal load 400 V, frequency 50 Hz for the nominal rotational speed of the inductor 214.3 rpm were prognosticated by design calculations.

The designed PM prototype generator was manufactured and tested using the drive system with a converter-controlled induction motor. The open-circuit and load characteristics for different rotational speeds were measured. The three-phase load as a resistive load or as a diode rectifier with resistive load were connected to the terminals of the PM generator.

The waveform of measured open-circuit phase-to-phase voltage of the PM generator at the rated speed of 214.3 rpm is shown in Fig. 12. The phase-to-phase voltages of the prototype PM generator are almost sinusoidal. The value

of open circuit depends on the temperature of magnets. The measured open-circuit phase-to-phase voltage is 493 V, and the calculated one is 488 V.

In the conditions of nominal three-phase symmetrical resistive load, the voltage of prototype PM generator is 405 V, the calculated one is 400 V. The computed data agree well with the experimentally measured ones. The differences may be caused by the magnet temperatures, which differ from the predicted ones. The waveform of measured voltage is almost sinusoidal (Fig. 13).
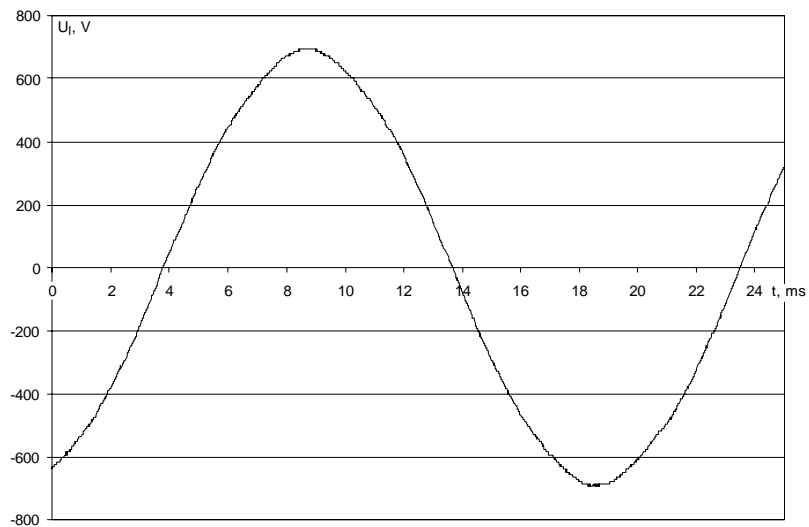

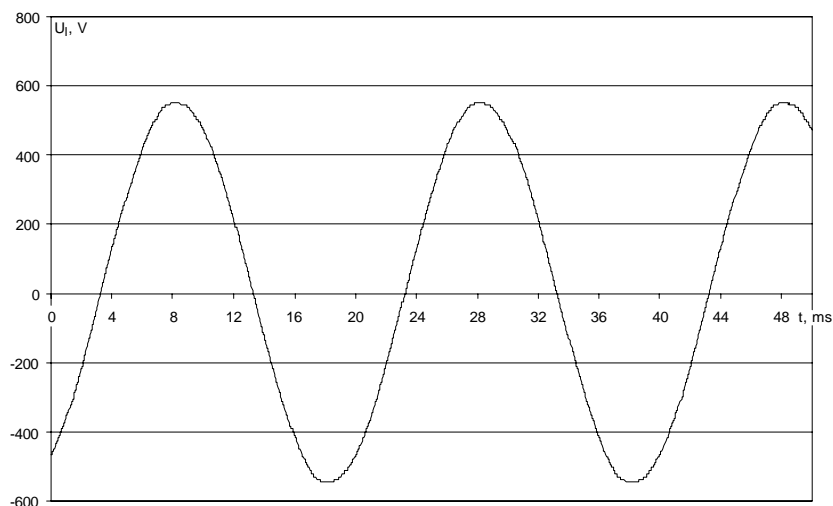*Fig. 12.* Open-circuit phase-to-phase voltage of the prototype PM generator.

Fig. 13. Phase-to-phase voltage of the prototype PM generator by three-phase symmetrical resistive load.

The waveform of phase-to-phase voltage by open-circuit or symmetrical three-phase resistive load is almost sinusoidal, but phase voltage has a significant influence due to the 3rd harmonic effects.

Conclusions and discussions

A 10 kW low-speed PM synchronous generator for wind power applications was designed and tested experimentally. A fractional two-layer armature winding was used to minimize the influence of ripple torque. NdFeB rectangular magnets were fixed into the nests on the surface of the inductor yoke. The analytical study of distribution of the primary magnetic field by conformal mapping and finite element methods was compared with experimental data of PM-model and prototype-machine tests. There was a relatively good correlation between the analytical and experimental data.

As a result of tests, a very low level of ripple torque as well as almost sinusoidal waveform and predicted level of line voltage were achieved. The calculated line voltages for no-load and different-load conditions tended to be lower than the experimentally measured voltages by 0.5–1.3%. It was caused mainly by the fact that experimental temperatures of magnets were relatively lower than calculated design temperatures.

The distribution of temperatures in different parts of winding, teeth and yoke zones of the stator core and permanent magnets has been calculated by the method of thermal network. The calculated temperatures and those measured by sensors experimentally correlated relatively well, differing less than by 5%. Development of more accurate methods of thermal analysis for PM machines will make it possible to achieve a more accurate level of electromagnetic analysis on the PM synchronous generators for wind power applications.

REFERENCES

1. European Wind Energy Association, Wind Force 12 – 2005. EWEA News Release, February 2006. http://ewea.org.
2. *Grauers, A*. Design of Direct-Driven Permanent-Magnet Generators for Wind Turbines // Technical Report no. 292, Chalmers University of Technology: Goteborg, Sweden, 1996. 133 pp.
3. *Lampola, P*. Directly Driven Low-Speed Permanent-Magnet Generators for Wind Power Applications // Ph.D. Dissertation, Helsinki University of Technology, Laboratory of Electromechanics: Espoo, Finland, 2000. 62 pp.
4. *Kilk, A*. Design and Experimental Verification of a Multipole Directly Driven Interior PM Synchronous Generator for Wind Power Applications // Proceedings of the 4th International Electric Power Quality and Supply Reliability Workshop: Pedase, Estonia, 2004. P. 87–89.

5. *Kilk, A*. Analysis of Permanent Magnet Multipole Synchronous Generators for Wind Applications // Proceedings of IEEE Compatibility in Power Electronics: Gdynia, Poland, 2005. P. 68–73.

6. *Lavrentjev, M., Shabat, B*. Theory and Methods of Complex Variable Functions. Moscow, 1965. 716 pp. [in Russian].